HHS Public Access

Author manuscript

RNA Biol. Author manuscript; available in PMC 2018 July 31.

Published in final edited form as:

RNA Biol. 2009 ; 6(1): 84–89.

Structure and activity of the internal ribosome entry site within the human p27^{Kip1} 5′-untranslated region

Jennifer Coleman[1,†] and **W. Keith Miskimins**[2,*]

[1]Division of Basic Biomedical Sciences; Sanford School of Medicine of the University of South Dakota; Vermillion, South Dakota USA

[2]Cancer Biology Research Center; Sanford Research/USD; Sioux Falls, South Dakota USA

Abstract

The cyclin dependent kinase inhibitor p27^{Kip1} is a key cell cycle regulatory protein that is often downregulated in cancer cells. The cellular levels of p27^{Kip1} are regulated, in part, through translational control mechanisms. The 5′-UTR of the p27^{Kip1} mRNA is known to harbor an IRES that may facilitate expression of p27^{Kip1} under conditions of stress such as loss of cell adhesion or growth factor and nutrient deprivation. The results presented here further characterize the p27^{Kip1} 5′-UTR and its IRES activity. We confirm that the major transcription start site of the p27^{Kip1} gene produces an mRNA with a 5′-UTR of ~472 nucleotides. Other minor transcripts are also observed but the 472 nucleotide 5′-UTR displays the highest IRES activity. A structural model for the 472 nucleotide 5′-UTR was derived from nuclease digestion patterns coupled with MFOLD secondary structural prediction software. These results indicate that the 5′-UTR has significant secondary structure but also contains a large single-stranded loop that extends from nucleotides -31 to -66 relative to the start codon. Mapping of the ribosome entry window indicates that the ribosome is recruited to this single-stranded loop. The single-stranded loop also includes a U-rich sequence that has previously been shown to bind several proteins, including HuR. This is significant because HuR has previously been shown to inhibit p27^{Kip1} IRES activity and cause downregulation of endogenous p27^{Kip1} protein levels. Thus HuR may inhibit IRES activity by blocking the ribosome entry site.

Keywords

p27^{Kip1}; IRES; 5′-UTR; cell cycle; RNA structure

Introduction

The protein p27^{Kip1} is a cyclin dependent kinase inhibitor that plays a key role in regulating cell cycle progression. Expression of p27^{Kip1} is high in quiescent cells and when cells are under various types of stress. Its expression is downregulated in proliferating cells and in most types of cancer.[1] The reduction of p27^{Kip1} in tumors is associated with poor clinical

*Correspondence to: W. Keith Miskimins; Cancer Biology Research Center; Sanford Research; University of South Dakota; Sioux Falls, South Dakota 57105 USA; keith.miskimins@usd.edu.

†Current address: AI duPont Hospital for Children; Nemours Biomedical Research; Wilmington, Delaware USA

outcome.[1] The cellular levels and activity of p27^{Kip1} are regulated at the levels of synthesis, degradation, subcellular localization and protein-protein interactions. For synthesis, translation of the p27^{Kip1} mRNA has been shown to be highest in quiescent cells[2–5] and to be upregulated during differentiation of certain cell types.[6,7] The proliferation-dependent increase in translation is controlled through the 5′-UTR of the p27^{Kip1} mRNA.[2,7–9] Various transcription start sites for the p27^{Kip1} gene have been described but the major start site produces a GC-rich 5′-UTR of 472 nucleotides.[10] The 5′-UTR has been shown to contain an internal ribosome entry site (IRES)[7,8,11–17] as well as an upstream open reading frame (uORF).[2] However, the start codon for the uORF is 519 nucleotides upstream of the p27^{Kip1} start codon and would not be present in the most abundant p27^{Kip1} mRNA.[2,10] The p27^{Kip1} 5′-UTR has also been shown to interact with several RNA-binding proteins, including HuR, HuD, hnRNP C and PTB.[8,9,12] HuR and HuD have been shown to inhibit IRES activity by interacting with a U-rich element located just upstream of the p27^{Kip1} start codon.[8] PTB, in constrast, has been shown to enhance IRES activity but the precise binding site for this protein is unknown.[12]

The process of ribosome recruitment through the p27^{Kip1} IRES and the mechanisms by which RNA-binding proteins modulate this process requires further characterization. In the work described here we have examined the usage of various transcriptional start sites in the *p27^{Kip1}* gene and determined the relative IRES activity of the resulting 5′-UTRs. Based on sensitivity to RNases we have developed a model for the structure of the p27^{Kip1} 5′-UTR. The data indicates that this region of the message has a large single-stranded loop embedded within extensive secondary structure and that the ribosome enters through this single-stranded region during translation initiation.

Results

The p27^{Kip1} mRNA containing a 472 nucleotide 5′-UTR is the most abundant p27^{Kip1} transcript expressed in cells

Previous work using 5′ RNA ligase-mediated RACE (5′ RLM-RACE) identified the major transcription initiation site of the human *p27^{Kip1}* gene at 472 base pairs upstream of the protein coding region.[10] Minor transcription start sites were also observed at 677, 403, 316 and 289 base pairs upstream of the protein coding region.[10] Various other transcription initiation sites have also been reported[9,18,19] and Hengst and coworkers[2,8] have described a transcription initiation site 575 base pairs upstream of the protein coding region. These authors showed that transcription initiation at this site produces an mRNA with an upstream open reading frame (uORF) that overlaps with a cell cycle regulatory element.[2] To provide a more accurate measure of the frequency of transcription start site usage on the human *p27^{Kip1}* gene, a ribonuclease protection assay using a longer probe was performed. A labeled antisense RNA probe was made using the cDNA sequence of the longest transcript previously identified.[10] The probe was 740 nucleotides in length, consisting of p27^{Kip1} sequence from 17 to 677 nucleotides upstream of the AUG with the remaining 79 nucleotides derived from non-p27 ^{Kip1} sequences. The labeled probe was hybridized with total RNA from the breast cancer cell line MCF7 or the non-transformed breast cell line MCF10A, followed by digestion with RNase and analysis of the protected RNAs on a

denaturing polyacrylamide gel. For both the transformed and non-transformed breast cell lines, a major band at approximately 450 nucleotides was observed (Fig. 1). This corresponds to the major transcription initiation site at 472 base pairs upstream of the protein coding region.[10] Faint bands were also observed below the 400 nucleotide marker and between the 500 and 740 nucleotide markers. This larger band may correspond to a start site 575 nucleotides upstream of the $p27^{Kip1}$ start codon that was described by Kullman et al.[8] Based on the data presented here and the previous RLM-RACE data,[10] it can be concluded that the major *p27Kip1* transcription start site produces a message with a 5′-UTR of 472 nucleotides.

The 472 nucleotide $p27^{Kip1}$ 5′-UTR has the highest level of IRES activity

It has been previously reported that both the mouse and human $p27^{Kip1}$ 5′-UTRs contain IRESs.[7,8,11–17] Since multiple transcription initiation sites resulting in transcripts containing 5′-UTRs of differing lengths have been identified, a comparison of the IRES activity of the different sizes of $p27^{Kip1}$ 5′-UTRs was made. Since the major transcription start site is 472 nucleotides upstream of the AUG start codon, the regions of the *p27Kip1* gene encoding the 575 and 677 base pair 5′-UTRs are expected to have promoter activity. This was confirmed experimentally (data not shown). It was therefore necessary to perform direct RNA transfections of bicistronic mRNAs to make an accurate comparison of the IRES activity of the 5′-UTR sequences. Capped and polyadenylated dual luciferase mRNAs with the various $p27^{Kip1}$ 5′-UTRs in the intercistronic region were transfected into breast cancer cell lines MDA-MB-231 and MCF7. After harvesting, Renilla and firefly luciferase activities were assayed and the firefly/Renilla ratio was calculated (Fig. 2). A transcript containing the 472 nucleotide $p27^{Kip1}$ 5′-UTR in reverse orientation was used as a negative control. While each $p27^{Kip1}$ 5′-UTR assayed contained some IRES activity, the IRES in the 472 nucleotide 5′-UTR was the most active (Fig. 2A and B).

The $p27^{Kip1}$ 472 nucleotide 5′-UTR contains a high degree of secondary structure and a large single-stranded loop

It is widely believed that the extensive structure of IRESs, both viral and cellular, creates a complex RNA scaffold that contains multiple sites for interactions with canonical initiation factors, IRES transacting factors (ITAFs) and 40S ribosomes.[20,21] Chemical and enzymatic probing coupled with computer prediction analysis has been used to model RNA secondary structures of several cellular IRESs, including c-myc, L-myc, Apaf-1, cat-1 and others.[22–27] These models reveal complex secondary structures which include stem-loops and possible pseudoknots. Although the mechanism is still unclear for how cellular IRESs promote internal ribosome entry, the importance of RNA structure has been shown. C-myc IRES function can be disabled by mutations or deletions that disrupt separate structural regions.[22] Disruption of RNA-RNA interactions between the 5′ and 3′ ends of the cat-1 IRES prevents inducible internal initiation, whereas restoration of this structural feature re-establishes activity.[26] Structural elements in the Apaf-1 IRES that are believed to provide binding sites for ITAFs have been identified and the altered conformation due to ITAF binding is suggested to create the ribosome entry site.[24] Since there is a strong relationship between the structure and the function of an IRES element, to fully understand the mechanism of action of an IRES it is important to determine its structural characteristics.

Enzymatic probing of the human p27^{Kip1} 472 nucleotide 5′-UTR was performed in order to obtain data to use in computer prediction analysis to derive secondary structure models of the human IRES. Capped RNA consisting of the human p27^{Kip1} 472 nucleotide 5′-UTR sequence plus an additional 20 nucleotides of non-p27^{Kip1} sequence at the 3′ end was subjected to cleavage by several different RNases. The cleaved RNA was then hybridized to end-labeled primers complementary to sequences in the p27^{Kip1} 5′-UTR or the additional 20 bases and reverse transcription was performed. The cleavage/reverse transcription products were run on urea-containing polyacrylamide gels with a sequencing reaction using the same labeled primer to orient the bands to the sequence. A portion of a gel representing the p27^{Kip1} polypyrimidine tract and the cleavage/ reverse transcription products is shown in Figure 3 as an example.

Single-stranded and double-stranded areas of the RNA were determined by the banding pattern after RNase cleavage and reverse transcription. RNase A cleaves primarily in single-stranded regions at pyrimidines (C and U). RNase T1 preferentially cleaves single-stranded G nucleotides. RNase One cleaves at every single-stranded nucleotide. Lastly, RNase V cleaves double-stranded RNAs. The cleavage and reverse transcription experiments were carried out 11 times with different combinations of RNases and different end-labeled primers. A spreadsheet was created to indicate the banding pattern at every base and this data was used as input parameters to force or inhibit pairing. The secondary structure prediction based on these parameters was generated using the web-based application MFOLD.[28,29] As expected, the 472 nucleotide p27^{Kip1} 5′-UTR contains a high degree of secondary structure (Fig. 4). However, another interesting feature of the 5′-UTR is a large single-stranded loop extending from -31 to -66 relative to the start codon. This loop contains a U-rich region that has previously been shown to interact with RNA-binding proteins, including the proteins HuR and HuD that have been shown to modulate p27 IRES activity.[8,9]

The U-rich single-stranded loop within the p27^{Kip1} 5′-UTR is important for ribosome recruitment

One of the major unanswered questions concerning cellular IRES elements is how they recruit the 40S ribosome and allow for its proper positioning.[20] To understand this, it will be important to determine the region of the p27^{Kip1} 5′-UTR where the ribosome enters during IRES-dependent initiation. To locate the ribosome entry window within the p27^{Kip1} 5′-UTR we introduced AUG initiation codons at various positions across the sequence using site-specific mutagenesis. Each of the introduced upstream AUGs was within a good Kozak consensus sequence[30] to ensure the possibility of translation initiation. The uORFs created by these AUGs are out of frame with the downstream firefly luciferase coding region and also overlaps this sequence. Thus, if the inserted AUG lies downstream of the ribosome entry site, synthesis will initiate at the uORF leading to a decrease in firefly luciferase expression. In contrast, if the ribosome entry site lies downstream of the introduced AUG there will be little or no change in firefly luciferase synthesis. This approach has previously been used to determine the ribosome binding window for cellular IRESs.[22,23] Bicistronic reporter constructs carrying the 472 nucleotide 5′-UTR with out-of-frame AUGs 11, 36, 50 or 74 nucleotides upstream of the 3′ end of the UTR (Fig. 5) were transfected into MCF7 cells. The IRES activity of the -50 and -74 AUG mutants was only slightly diminished from

that of wild type. In contrast, the -11 and -36 AUG mutant constructs retained only 36% and 42%, respectively, of wild type activity. This indicates that while the mutant AUGs at 50 and 74 nucleotides upstream were frequently bypassed, the mutant AUGs at 36 and 11 nucleotides upstream were frequently used by the ribosome. These experiments support the conclusion that the ribosome enters between 36 and 50 nucleotides upstream of the $p27^{Kip1}$ start codon for IRES-initiated translation. Interestingly, this is within the U-rich region that forms a large single-stranded loop (see Fig. 4).

Discussion

Various transcription start sites, ranging from 153 to 677 nucleotides upstream of the AUG start codon, have been reported for the human *p27Kip1* gene.[8–10,18,19] However, using 5′ RLM-RACE, a precise method of determining authentic capped 5′ ends of mRNAs, it was shown that the major transcription start site for human *p27Kip1* produces a 472 nucleotide 5′-UTR.[10] The results presented here confirm that the overwhelming majority of $p27^{Kip1}$ transcripts, at least in MCF7 and MCF10A cells, have a 5′-UTR in this size range. In addition transcripts with the 472 nucleotide 5′-UTR display the highest level of IRES activity. Lengthening the 5′-UTR to 575 or 677 nucleotides or shortening it to 403 nucleotides reduces IRES activity. These effects are possibly due to changes in secondary structure or RNA-protein interactions. Gopfert et al.[2] identified an element that overlaps an uORF within the $p27^{Kip1}$ 5′-UTR that enhances translation in a cell cycle-dependent manner. The start codon for the uORF is 519 nucleotides upstream of the start codon for the $p27^{Kip1}$ protein. Thus, neither the uORF nor the cell cycle regulatory element is present in the major $p27^{Kip1}$ transcript. We did detect a very small percentage of transcripts that have longer 5′-UTRs and the uORF and cell cycle regulatory element may play a role in regulating translation of these transcripts.

Based on RNase digestion patterns a model of secondary structure within the $p27^{Kip1}$ 5′-UTR was established. This region is predicted to have extensive secondary structure with a large single-stranded loop located just upstream of the translation start codon. The ribosome entry window for IRES-mediated translation initiation maps to the large single-stranded loop. This region includes a U-rich element that has been shown to be necessary for binding to HuR and HuD,[8,9] RNA-binding proteins of the ELAV family. HuR and HuD have been shown to inhibit $p27^{Kip1}$ IRES activity.[8] One possibility is that ELAV proteins bind to the U-rich single-stranded loop to block recruitment of the initiation complex. Elevated cytoplasmic expression of HuR has been linked to carcinogenesis and is associated with reduced survival in breast, ovarian and gastric adenocarcinomas.[31–37] It is therefore possible that HuR binding to the $p27^{Kip1}$ 5′-UTR contributes to its role in cancer progression. In addition to the single-stranded loop it is likely that the potential of the $p27^{Kip1}$ 5′-UTR to form extensive secondary structures is important for IRES activity. It is possible that other 5′-UTR-binding proteins, such as PTB,[12] stabilize a structure that facilitates ribosome recruitment and thus enhances expression of $p27^{Kip1}$.

Materials and Methods

Cells lines and DNA constructs

Human breast cancer cell lines MDA-MB-231 and MCF7 and human non-transformed breast cell line MCF10A were maintained in a humidified atmosphere containing 5% CO_2 in Dulbecco's modified Eagle's medium with 10% fetal bovine serum, 100 U/ml penicillin and 100 μg/ml streptomycin.

The human $p27^{Kip1}$ 5′-UTRs of 403, 472, 575 and 677 base pairs in length were cloned into the dual luciferase reporter plasmid pTKLL at the intercistronic HindIII site.[14]

Ribonuclease protection assay

A probe was made using the MAXIscript kit (Ambion), ^{32}P-CTP, and T7 RNA polymerase. DNA from a TOPO clone containing the human *p27Kip1* sequence from -677 to -17 (relative the AUG start codon) was linearized with Pme I and used as a template for probe synthesis. After gel purification of the probe, the assay was carried out using the HybSpeed RPA kit (Ambion) as per kit protocol. Total RNA, extracted using TRI Reagent (Molecular Research), was co-precipitated with the labeled probe followed by denaturation and hybridization. Following digestion with RNase A/T1, the protected RNAs were precipitated, resuspended and run on a 4% denaturing polyacrylamide gel with ^{32}P-labeled Century markers (Ambion) and then detected by autoradiography.

In vitro transcription of RNA for transfection and cleavage

Bicistronic DNA templates for in vitro transcription were amplified using the Advantage 2 PCR kit (BD Biosciences). The pTKLL vectors containing the $p27^{Kip1}$ 5′-UTRs of differing lengths were used as templates for PCR. The 5′ primers contained T7 5′ overhangs followed by sequence specific to Renilla luciferase (GGA TCC TAA TAC GAC TCA CTA TAG GGA GTT CAA TTA CAG CTC TTA) and the 3′ primer contained a 30 nucleotide 3′ overhang to create a polyA tail (T_{30}AGC TAA GAA TTT CGT CAT CG). Templates were gel purified on a 1% agarose gel.

DNA templates for in vitro transcription containing a T7 promoter and the human 472 bp 5′-UTR sequence with 20 additional bases of vector sequence at the 3′ end were also amplified using the Advantage 2 PCR kit. Vector pGL2CAT/Luc containing the human 472 bp 5′-UTR sequence was used as a template. The 5′ primer contained a T7 5′ overhang followed by sequence specific to the 5′ end of the UTR (GGA TCC TAA TAC GAC TCA CTA TAG GCT TCT TCG TCA GCC TCC CTT). The 3′ primer contained sequence from the vector immediately downstream of the 5′-UTR (CCA TTT TAC CAA CAG TAC CGG).

Bicistronic mRNAs containing a 7-methylguanosine (7mG) cap for transfection were made using the Message Machine kit (Ambion). One microgram of the gel-purified templates was used per reaction. After DNase digestion, the RNA was extracted, precipitated and resuspended in Secure Resuspension Solution (Ambion). The human 472 nucleotide 5′-UTR was also transcribed using the Message Machine kit as described to obtain a 7mG-capped RNA for use in cleavage experiments.

DNA and RNA transfections and luciferase assays

Cells were transfected with DNA using GenePorter (Gene Therapy Systems) transfection reagent. Three micrograms of DNA and 4 μl of GenePorter were used per 35 mm culture dish in serum-free medium. Four hours after transfection, the medium was replaced with medium containing 10% fetal calf serum. Cells were harvested one day after transfection by rinsing with PBS followed by addition of 150 μl of reporter lysis buffer (Promega) and scraping the cells from the bottom of the dish.

Cells were transfected with mRNAs using DMRIE-C transfection reagent (Invitrogen). Cells in 35 mm dishes were rinsed with serum-free medium to remove any antibiotics. DMRIE-C and then mRNA were added to 1 ml of serum-free medium at a ratio of 2 μl DMRIE-C:1 μg mRNA. The mixture was vortexed and immediately applied to the cells. Four hours after transfection, the medium was replaced with medium containing 10% fetal bovine serum. The cells were incubated six additional hours and then harvested in 100 μl reporter lysis buffer.

Luciferase activity was determined using the Dual-Glo Luciferase Assay System (Promega) for both Renilla and firefly luciferase activities using 50–100 μl of cellular extract.

RNA cleavage and reverse transcription

DNA primers for reverse transcription were end-labeled by incubating 50 pmol each of primer and **γ**-^{32}P-ATP with T4 polynucleotide kinase in a total reaction volume of 50 **μ**l. The end-labeled primers were gel purified on a 5% polyacrylamide gel containing urea. The labeled primers were visualized by autoradiography, excised and eluted.

The capped p27^{Kip1} 472 nucleotide 5′-UTR RNA (~1 pmol per 100 **μ**l reaction) was incubated in cleavage buffer (10 mM Tris-HCl pH 7.5, 10 mM magnesium chloride and 50 mM potassium chloride) and cleaved with empirically derived amounts of RNase A, RNase T1, RNase V or RNase One. Reactions were stopped by phenol/chloroform extraction followed by ethanol precipitation.

Reverse transcription of the cleaved RNA was done using AMV RT (Promega). The pellet of cleaved RNA was resuspended in 4 **μ**l RT buffer and annealed to the labeled primers at 65°C for five minutes. Extension was then carried out using 0.5 U AMV RT per reaction (in RT buffer with 12 mM DTT and 0.6 mM dNTPs per reaction) at 42°C for 30 minutes. After RNase digestion with 2 **μ**g RNase A for 30 minutes at 37°C to remove the template RNA, the reactions were subjected to phenol/chloroform extraction and ethanol precipitation. For orientation of the cleavage products to the sequence, sequencing reactions were carried out with the USB Sequenase version 2.0 DNA sequencing kit (Amersham) using end-labeled primers with the pGL2CAT/Luc vector containing the 472 bp 5′-UTR sequence as template. All reverse transcription and sequencing samples were run on urea-containing 8% polyacrylamide gels. The gels were dried and the bands were visualized by autoradiography.

Secondary structure prediction

Banding patterns on the sequencing gels were used to determine areas of single- and doublestrandedness. These data were used as folding parameters to force or prohibit pairing of nucleotides in the $p27^{Kip1}$ 5′-UTR. The secondary structure prediction based on these parameters was generated using the web-based application MFOLD at www.bioinfo.rpi.edu/applications/mfold.

Site-directed mutagenesis

For site-directed mutagenesis, pcDNA3.1LUC plasmids containing the 472 bp $p27^{Kip1}$ 5′-UTR were amplified using Pfu polymerase (Stratagene) and complementary primers containing 1–3 mutated bases to create ATG start codons within the 5′-UTR. After PCR, reactions were digested with Dpn I to remove the parental template and the resultant plasmids were transformed into One Shot Top 10 cells (Invitrogen). The DNA was sequenced at the Iowa State Sequencing Facility to verify the mutations. The mutated 5′ UTRs were then subcloned into the intercistronic Hind III site of the pTKLL bicistronic reporter construct for testing.

Acknowledgments

This work was supported by a grant from the US Public Health Service, National Cancer Institute R01CA084325.

Abbreviations

IRES	internal ribosome entry site
UTR	untranslated region
ORF	open reading frame
PTB	polypyrimidine-tract binding protein
RACE	rapid amplification of cDNA ends
ITAF	IRES trans-acting factor

References

1. Chu IM, Hengst L, Slingerland JM. The Cdk inhibitor p27 in human cancer: prognostic potential and relevance to anticancer therapy. Nat Rev Cancer. 2008; 8:253–67. [PubMed: 18354415]
2. Gopfert U, Kullmann M, Hengst L. Cell cycle-dependent translation of p27 involves a responsive element in its 5′-UTR that overlaps with a uORF. Hum Mol Genet. 2003; 12:1767–79. [PubMed: 12837699]
3. Hengst L, Reed SI. Translational control of $p27^{Kip1}$ accumulation during the cell cycle. Science. 1996; 271:1861–4. [PubMed: 8596954]
4. Agrawal D, Hauser P, McPherson F, Dong F, Garcia A, Pledger WJ. Repression of $p27^{kip1}$ synthesis by platelet-derived growth factor in BALB/c 3T3 cells. Mol Cell Biol. 1996; 16:4327–36. [PubMed: 8754833]
5. Vidal A, Millard SS, Miller JP, Koff A. Rho activity can alter the translation of p27 mRNA and is important for RasV12-induced transformation in a manner dependent on p27 status. J Biol Chem. 2002; 277:16433–40. [PubMed: 11875067]

6. Millard SS, Yan JS, Nguyen H, Pagano M, Kiyokawa H, Koff A. Enhanced ribosomal association of p27(Kip1) mRNA is a mechanism contributing to accumulation during growth arrest. J Biol Chem. 1997; 272:7093–8. [PubMed: 9054402]
7. Miskimins WK, Wang G, Hawkinson M, Miskimins R. Control of cyclin-dependent kinase inhibitor p27 expression by cap-independent translation. Mol Cell Biol. 2001; 21:4960–7. [PubMed: 11438653]
8. Kullmann M, Gopfert U, Siewe B, Hengst L. ELAV/Hu proteins inhibit p27 translation via an IRES element in the p27 5′UTR. Genes Dev. 2002; 16:3087–99. [PubMed: 12464637]
9. Millard SS, Vidal A, Markus M, Koff A. A U-rich element in the 5′ untranslated region is necessary for the translation of p27 mRNA. Mol Cell Biol. 2000; 20:5947–59. [PubMed: 10913178]
10. Coleman J, Hawkinson M, Miskimins R, Miskimins WK. The major transcription initiation site of the $p27^{Kip1}$ gene is conserved in human and mouse and produces a long 5′-UTR. BMC Mol Biol. 2001; 2:12. [PubMed: 11696240]
11. Chaudhuri S, Vyas K, Kapasi P, Komar AA, Dinman JD, Barik S, Mazumder B. Human ribosomal protein L13a is dispensable for canonical ribosome function but indispensable for efficient rRNA methylation. RNA. 2007; 13:2224–37. [PubMed: 17921318]
12. Cho S, Kim JH, Back SH, Jang SK. Polypyrimidine tract-binding protein enhances the internal ribosomal entry site-dependent translation of $p27^{Kip1}$ mRNA and modulates transition from G_1 to S phase. Mol Cell Biol. 2005; 25:1283–97. [PubMed: 15684381]
13. Jiang H, Coleman J, Miskimins R, Miskimins WK. Expression of constitutively active 4EBP-1 enhances $p27^{Kip1}$ expression and inhibits proliferation of MCF7 breast cancer cells. Cancer Cell Int. 2003; 3:2. [PubMed: 12633504]
14. Jiang H, Coleman J, Miskimins R, Srinivasan R, Miskimins WK. Cap-independent translation through the p27 5′-UTR. Nucleic Acids Res. 2007; 35:4767–78. [PubMed: 17617641]
15. Shi Y, Sharma A, Wu H, Lichtenstein A, Gera J. Cyclin D1 and c-myc internal ribosome entry site (IRES)-dependent translation is regulated by AKT activity and enhanced by rapamycin through a p38 MAPK- and ERK-dependent pathway. J Biol Chem. 2005; 280:10964–73. [PubMed: 15634685]
16. Wilker EW, van Vugt MA, Artim SA, Huang PH, Petersen CP, Reinhardt HC, Feng Y, Sharp PA, Sonenberg N, White FM, Yaffe MB. 14-3-3sigma controls mitotic translation to facilitate cytokinesis. Nature. 2007; 446:329–32. [PubMed: 17361185]
17. Yoon A, Peng G, Brandenburger Y, Zollo O, Xu W, Rego E, Ruggero D. Impaired control of IRES-mediated translation in X-linked dyskeratosis congenita. Science. 2006; 312:902–6. [PubMed: 16690864]
18. Ito E, Iwahashi Y, Yanagisawa Y, Suzuki Y, Sugano S, Yuasa Y, Maruyama K. Two short sequences have positive effects on the human $p27^{Kip1}$ gene transcription. Gene. 1999; 228:93–100. [PubMed: 10072762]
19. Minami S, Ohtani-Fujita N, Igata E, Tamaki T, Sakai T. Molecular cloning and characterization of the human $p27^{Kip1}$ gene promoter. FEBS Lett. 1997; 411:1–6. [PubMed: 9247132]
20. Komar AA, Hatzoglou M. Internal ribosome entry sites in cellular mRNAs: mystery of their existence. J Biol Chem. 2005; 280:23425–8. [PubMed: 15749702]
21. Stoneley M, Willis AE. Cellular internal ribosome entry segments: structures, transacting factors and regulation of gene expression. Oncogene. 2004; 23:3200–7. [PubMed: 15094769]
22. Le Quesne JP, Stoneley M, Fraser GA, Willis AE. Derivation of a structural model for the c-myc IRES. J Mol Biol. 2001; 310:111–26. [PubMed: 11419940]
23. Jopling CL, Spriggs KA, Mitchell SA, Stoneley M, Willis AE. L-Myc protein synthesis is initiated by internal ribosome entry. RNA. 2004; 10:287–98. [PubMed: 14730027]
24. Mitchell SA, Spriggs KA, Coldwell MJ, Jackson RJ, Willis AE. The Apaf-1 internal ribosome entry segment attains the correct structural conformation for function via interactions with PTB and unr. Mol Cell. 2003; 11:757–71. [PubMed: 12667457]
25. Fernandez J, Yaman I, Huang C, Liu H, Lopez AB, Komar AA, Caprara MG, Merrick WC, Snider MD, Kaufman RJ, Lamers WH, Hatzoglou M. Ribosome stalling regulates IRES-mediated translation in eukaryotes, a parallel to prokaryotic attenuation. Mol Cell. 2005; 17:405–16. [PubMed: 15694341]

26. Yaman I, Fernandez J, Liu H, Caprara M, Komar AA, Koromilas AE, Zhou L, Snider MD, Scheuner D, Kaufman RJ, Hatzoglou M. The zipper model of translational control: a small upstream ORF is the switch that controls structural remodeling of an mRNA leader. Cell. 2003; 113:519–31. [PubMed: 12757712]
27. Martineau Y, Le Bec C, Monbrun L, Allo V, Chiu IM, Danos O, Moine H, Prats H, Prats AC. Internal ribosome entry site structural motifs conserved among mammalian fibroblast growth factor 1 alternatively spliced mRNAs. Mol Cell Biol. 2004; 24:7622–35. [PubMed: 15314170]
28. Mathews DH, Turner DH, Zuker M. RNA secondary structure prediction. Curr Protoc Nucleic Acid Chem. 2007; 11:11–2.
29. Zuker M. Mfold web server for nucleic acid folding and hybridization prediction. Nucleic Acids Res. 2003; 31:3406–15. [PubMed: 12824337]
30. Kozak M. An analysis of 5′-noncoding sequences from 699 vertebrate messenger RNAs. Nucleic Acids Res. 1987; 15:8125–48. [PubMed: 3313277]
31. Stoppoloni D, Cardillo I, Verdina A, Vincenzi B, Menegozzo S, Santini M, Sacchi A, Baldi A, Galati R. Expression of the embryonic lethal abnormal vision-like protein HuR in human mesothelioma: association with cyclooxygenase-2 and prognosis. Cancer. 2008
32. Niesporek S, Kristiansen G, Thoma A, Weichert W, Noske A, Buckendahl AC, Jung K, Stephan C, Dietel M, Denkert C. Expression of the ELAV-like protein HuR in human prostate carcinoma is an indicator of disease relapse and linked to COX-2 expression. Int J Oncol. 2008; 32:341–7. [PubMed: 18202756]
33. Heinonen M, Fagerholm R, Aaltonen K, Kilpivaara O, Aittomaki K, Blomqvist C, Heikkila P, Haglund C, Nevanlinna H, Ristimaki A. Prognostic role of HuR in hereditary breast cancer. Clin Cancer Res. 2007; 13:6959–63. [PubMed: 18056170]
34. Mrena J, Wiksten JP, Kokkola A, Nordling S, Haglund C, Ristimaki A. Prognostic significance of cyclin A in gastric cancer. Int J Cancer. 2006; 119:1897–901. [PubMed: 16708383]
35. Erkinheimo TL, Sivula A, Lassus H, Heinonen M, Furneaux H, Haglund C, Butzow R, Ristimaki A. Cytoplasmic HuR expression correlates with epithelial cancer cell but not with stromal cell cyclooxygenase-2 expression in mucinous ovarian carcinoma. Gynecol Oncol. 2005; 99:14–9. [PubMed: 16126263]
36. Heinonen M, Bono P, Narko K, Chang SH, Lundin J, Joensuu H, Furneaux H, Hla T, Haglund C, Ristimaki A. Cytoplasmic HuR expression is a prognostic factor in invasive ductal breast carcinoma. Cancer Res. 2005; 65:2157–61. [PubMed: 15781626]
37. Erkinheimo TL, Lassus H, Sivula A, Sengupta S, Furneaux H, Hla T, Haglund C, Butzow R, Ristimaki A. Cytoplasmic HuR expression correlates with poor outcome and with cyclooxygenase 2 expression in serous ovarian carcinoma. Cancer Res. 2003; 63:7591–4. [PubMed: 14633672]

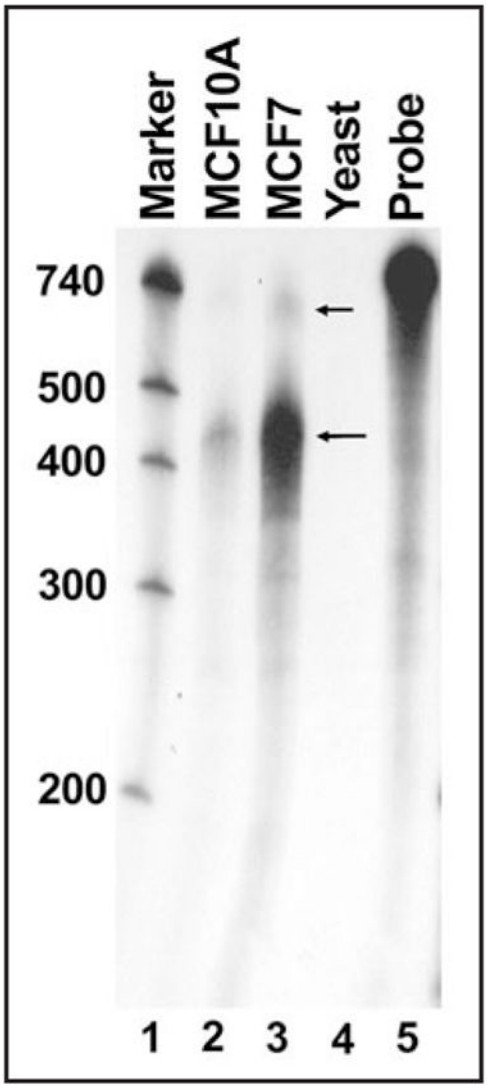

Figure 1.

Transcription start site mapping by RNase protection analysis of human $p27^{Kip1}$ mRNA. An RNase protection assay was performed using $p27^{Kip1}$ mRNA derived from MCF10A (lane 2) or MCF7 (lane 3) cells. The intact probe (lane 5) was 740 bases in length including $p27^{Kip1}$ sequences from 17 to 677 nucleotides upstream of the AUG and 79 nucleotides derived from vector sequence. Molecular marker size (in nucleotides, lane 1) is indicated on the left. The large arrow indicates the major protected fragment corresponding to the 472 nucleotide $p27^{Kip1}$ 5′-UTR and the small arrow indicates a larger, minor protected fragment corresponding to a ~575 nucleotide 5′-UTR. A control reaction using RNA derived from yeast is shown (lane 4).

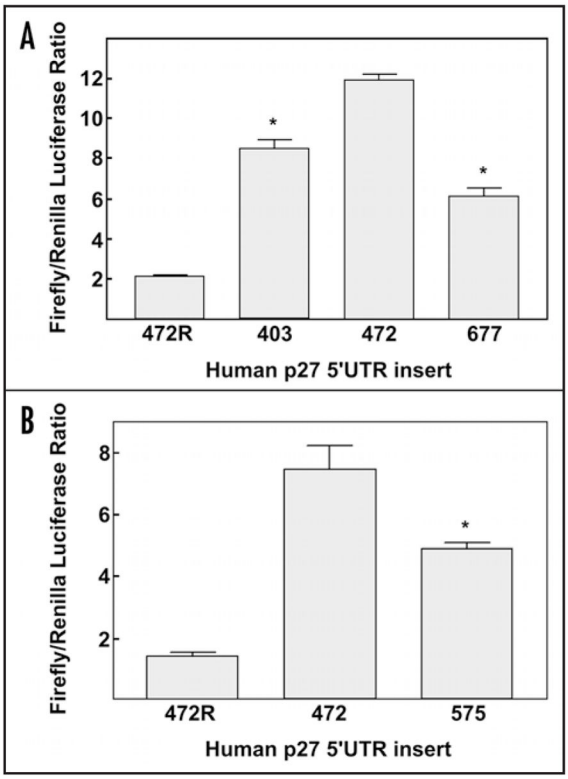

Figure 2.

The 472 nucleotide p27^{Kip1} 5′-UTR contains the highest IRES activity. Direct RNA transfections of bicistronic dual luciferase mRNAs containing the p27^{Kip1} 5′-UTRs were performed using DMRIE-C transfection reagent. Cells were harvested ten hours after transfection followed by assays for Renilla and firefly luciferase activity levels (in relative light units) and calculation of the firefly/Renilla ratio. (A) Transfection of MDA-MB-231 cells with RNAs containing the 677, 472 and 403 nucleotide p27^{Kip1} 5′-UTRs. A negative control transfection with an RNA transcript containing the reverse complement of the 472 nucleotide 5′-UTR was also performed (472R). Asterisks indicate statistically significant reduction in firefly/Renilla ratio relative to the 472 nucleotide 5′-UTR (unpaired t test; p = 0.0022 for the 403 nucleotide 5′-UTR; p = 0.00021 for the 677 nucleotide 5′-UTR). (B) Transfection of MCF7 cells with RNAs containing the 472 and 575 nucleotide p27^{Kip1} 5′-UTRs and the 472R negative control. Asterisk indicates statistically significant reduction in firefly/Renilla ratio relative to the 472 nucleotide 5′-UTR (unpaired t test; p = 0.03 for the 575 nucleotide 5′-UTR).

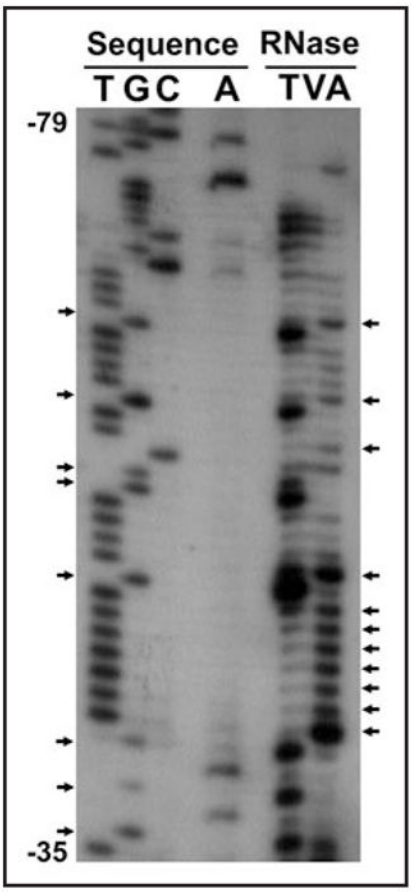

Figure 3.

Cleavage/reverse transcription products determine areas of single- and double-strandedness. Sequencing and cleavage/RT reactions were carried out with a primer complementary to the 3′ end of the p27^{Kip1} 5′-UTR and run on an 8% urea-containing polyacrylamide gel. Sample area demonstrates the results seen in the area of the human p27 ^{Kip1} 5′-UTR polypyrimidine tract. Arrows on the left point out G's in the sequence that are cleaved by RNase T and are therefore single-stranded. Arrows on the right point out C's and T's in the sequence that are cleaved by RNase A and are also therefore single-stranded.

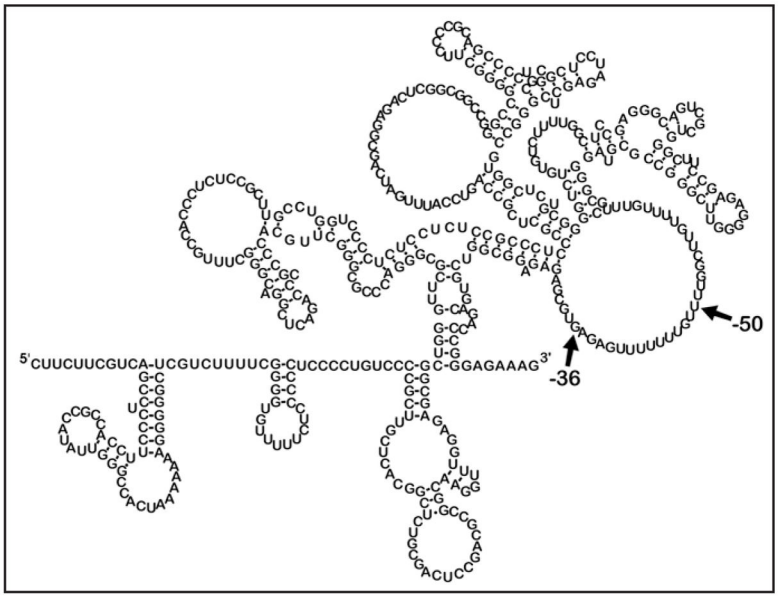

Figure 4.

MFOLD secondary structure prediction for the 472 nucleotide p27^{Kip1} 5′-UTR. Banding patterns seen after cleavage/RT (as in Fig. 3) were used to identify areas of single- and doublestrandedness of the p27^{Kip1} 472 nucleotide 5′-UTR. Based on these input parameters which forced or prohibited pairing, the MFOLD application predicted this complex secondary structure. The 5′ and 3′ ends of the 5′-UTR are indicated. The region between -36 and -50 indicate the proposed ribosome entry window for IRES-mediated initiation of translation (see Fig. 5).

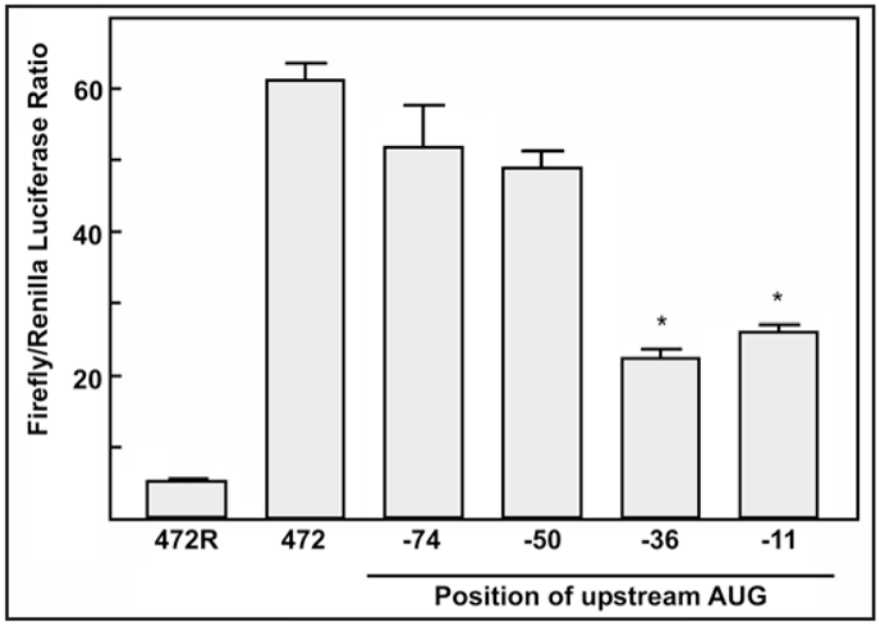

Figure 5.

Ribosome entry window for IRES-initiated translation is between 36 and 50 nucleotides upstream of the $p27^{Kip1}$ start codon. DNA transfections of MCF7 cells with the dual luciferase constructs containing the 472 base 5′-UTR sequence with the mutated upstream AUGs were done with GenePorter transfection reagent. Cells were harvested one day after transfection followed by assays for Renilla and firefly luciferase activity levels (in relative light units) and calculation of the firefly/Renilla ratio. Asterisks indicate statistically significant reduction in firefly/Renilla ratio relative to the wild-type control ($p < 0.001$).